Available online at www.sciencedirect.com
SCIENCE DIRECT
Biochimica et Biophysica Acta 1758 (2006) 573–582
BIOCHIMICA ET BIOPHYSICA ACTA
BBA
http://www.elsevier.com/locate/bba

The effect of calcium on the properties of charged phospholipid bilayers

Ulf R. Pedersen [a], Chad Leidy [b,1], Peter Westh [a], Günther H. Peters [b,*]

[a] Department of Life Science and Chemistry, Roskilde University, MEMPHYS-Center for Biomembrane Physics, 1 Universitetsvej, DK-4000 Roskilde, Denmark
[b] Department of Chemistry, Technical University of Denmark, MEMPHYS-Center for Biomembrane Physics, DK-2800 Lyngby, Denmark

Received 13 July 2005; received in revised form 8 March 2006; accepted 14 March 2006
Available online 19 April 2006

Abstract

We have performed molecular dynamics simulations to investigate the structure and dynamics of charged bilayers as well as the distribution of counterions at the bilayer interface. For this, we have considered the negatively charged di-myristoyl-phosphatidyl-glycerol (DMPG) and di-myristoyl-phosphatidyl-serine (DMPS) bilayers as well as a protonated di-myristoyl-phosphatidyl-serine (DMPSH) bilayer. We were particularly interested in calcium ions due to their important role in biological systems. Simulations performed in the presence of calcium ions (DMPG, DMPS) or sodium ions (DMPS) were run for 45–60 ns. Simulation results for DMPG are compared with fluorescence measurements. The average areas per molecule were 47.4±0.5 Å^2 (DMPG with calcium), 47.3±0.5 Å^2 (DMPS with calcium), 51.3±1.0 Å^2 (DMPS with sodium) and 45.3±0.5 Å^2 (DMPSH). The structure of the negatively charged lipids is significantly affected by the counterions, where calcium ions have a more pronounced effect than sodium ions. Calcium ions were found to be tightly bound to the anionic groups of the lipid molecules and as such appear to constitute an integral part of the membrane interface on nanoseconds time scales. In contrast to sodium ions, calcium ions are localised in a narrow (~10 Å) band around the phosphate group. The interaction of calcium with the lipid molecules enhances the molecular packing of the PG and PS lipids. This observation is in good agreement with emission spectra of the membrane partitioning probe Laurdan in DMPG multilamellar vesicles that indicate an increase in the ordering of the DMPG bilayer due to the presence of calcium. Our results indicate that calcium ions, which often function as a second messengers in living cells have a pronounced effect on membrane structures, which may have implications during signal transduction events.

Keywords: Molecular dynamics simulation; Fluorescence spectroscopy; DMPG; DMPS; Lipid order; Ion distribution; Membranes

1. Introduction

Biological membranes are essential for the integrity of the cell, providing a barrier between the inside and outside environments. They serve as the matrix and support for a vast array of proteins, which are involved in important functions of the cell such as energy transduction, signal transduction, solute transport, DNA replication, cell–cell recognition, protein targeting and trafficking [1]. In the traditional fluid mosaic model of biological membrane structure, bilayer lipids form a uniform and homogenous fluid mixture [2]. Consequently, the lipid membrane has long been considered as a two-dimensional solvent phase for membrane proteins. This prevailing view has been considerably refined during the past decade taking into account physicochemical studies of membrane lipids. A growing body of evidence has led to a picture, where the membrane structure plays an important role in signal transduction events and cellular restructuring processes. Lipid raft domains, hydrophobic mismatch, and membrane phospholipid asymmetry are a few examples of specific mechanisms by which membranes can take part in cellular events [3–11]. Hence, membranes play an active role in guiding lateral segregation of proteins [12–15], inducing the formation of domains that among other things offer a platform for the assembly of protein aggregates [1,6,16] and regulating/affecting protein activity [17] through changes in the membrane structural properties such as the main phase transition [18]. To unravel the complexity and to understand the response of a membrane due to external environmental stimuli on a molecular level, simpler ("model") systems have to be

* Corresponding author. Tel.: +45 4525 2486; fax: +45 4588 3136.
E-mail address: ghp@kemi.dtu.dk (G.H. Peters).
[1] Present address: Department of Physics, Universidad de los Andes, A.A. 4976 Bogota, Colombia.

0005-2736/$ - see front matter © 2006 Elsevier B.V. All rights reserved.
doi:10.1016/j.bbamem.2006.03.035

considered [19]. Although it is experimentally difficult to probe membrane properties on a molecular level, recent advances in single-molecule force and fluorescence spectroscopy have allowed to manipulate single molecules while simultaneously monitoring the response using a fluorescence probe [20,21]. These single molecule force experiments yield important information on structure-related mechanical properties, but do not provide information on the atomic-level [21]. Molecular dynamics (MD) simulation, on the other hand, provides information about membrane structure and dynamics [22]. The bilayer systems most intensively studied by MD simulations are phosphatidyl-choline (PC) lipid membranes, which have a zwitterionic head group. This is due to the fact that PC is an abundant and essential membrane phospholipid present in all eukaryotes. Early MD studies focused on homogeneous membranes, however in recent years, as a result of a rapid increase in computational power, simulations have been applied to systems of increasing complexibility [23,24]. These systems involve multicomponent lipid mixtures [25], bilayers interacting with monovalent ions [19,26,27], peptides [28], alcohol [29], sterols [30–35], disaccharides [36] and transmembrane proteins [37–41].

Molecular dynamics simulations consisting of negatively charged lipid bilayers have drawn less attention. This is surprising, since negatively charged lipid membranes consisting of phosphatidyl-glycerol (PG) or phosphatidyl-serine (PS) play a distinct functional role in maintaining membrane morphology and/or participating in signal transduction cascades [42–44]. PS is the major anionic phospholipid in most mammalian cell membranes and is predominantly found in the peripheral and central nervous system myelin, blood erythrocytes, and platelets. PS is involved in the upkeep and restoration of nerve cell membranes and the synapses, where it aids in cell-to-cell communication [45]. PG, on the other hand, is present in great abundance in both the plasma membrane of microorganisms and in the chloroplast membranes of green plants. In mammalian cells, PG occurs in minor amounts and is predominately found in mitochondrial membranes as well as in pulmonary surfactants [44,46]. Due to their anionic character at physiological pH, their phase transition behaviour is responsive to changes in the ionic environment. This provides a potential mechanism for regulating membrane structure triggered by changes in surface pH or concentration of monovalent and divalent ions [47–50].

In the present study, we investigate the effect of counterions (in particular the effect of divalent calcium ions) on the structure and dynamics of negatively charged di-myristoyl-phosphatidyl-glycerol (DMPG) and di-myristoyl-phosphatidyl-serine (DMPS) bilayers. Of particular interest is the distribution of calcium ions on the negatively charged membrane surfaces. We also considered a bilayer of di-myristoyl-phosphatidyl-serine, which was protonated on the carboxylate group (zwitterionic bilayer; hereafter referred to DMPSH) to study lipid–lipid interactions. The latter simulation was carried out without counter ions. A detailed insight into the structural behaviour of these homogeneous one-component membranes is essential, before advancing to more complex systems involving for instance enzyme–membrane complexes.

2. Material and methods

2.1. Molecular dynamics simulations

The initial structure of the anionic di-myristoyl-phosphatidyl-glycerol (DMPG; Fig. 1) and di-myristoyl-phosphatidyl-serine (DMPS; Fig. 1) bilayers were built from an equilibrated di-palmitoyl-phosphatidyl-choline (DPPC) bilayer [28] by deleting the methyl group and the first methylene group following the methyl group from each DPPC lipid. The gap between the two leaflets was reduced by moving the two leaflets closer together using the graphical program: Visualisation Molecular Dynamics (VMD) [51]. The missing hydrogen atoms on the terminal methylene group were automatically generated by the program psfgen [52]. The structure of the PS head group is very similar to that of the PC head group with the exception that PS has an additional

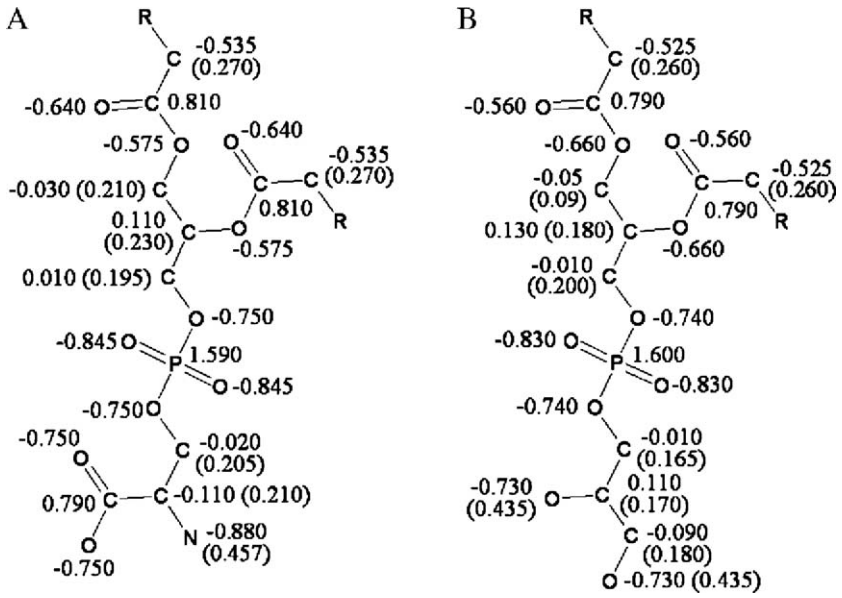

Fig. 1. Chemical structures of phosphatidyl-serine (A) and phosphatidyl-glycerol (B). The partial charges shown on the structure are based on ab initio calculation using the Restricted Hartree-Fock approximation with the 6-31+G* basis set. Numbers in parenthesis refer to partial charges on hydrogen atoms. See text for more details.

carboxylate group and the methyl groups on the nitrogen are replaced by hydrogen atoms (see Fig. 1). The carboxylate group was generated by replacing a hydrogen on the methylene group following the NH_3^+ group with a carboxylate group using psfgen [52]. The PG head group was built by replacing the $-N(CH_3)_3$ group in PC with a $-C(OH)H_2$ group. Additionally, a hydrogen on the methylene group following the NH_3^+ group was replaced by an oxygen. Missing hydrogen atoms were generated using psfgen [52]. Each bilayer consisting of 128 lipids (64 in each leaflet) was solvated using the program SOLVATE [53]. 64 water molecules were chosen randomly and replaced with calcium ions to neutralise the DMPG and DMPS systems. For the DMPS–Na^+ system, 128 water molecules were chosen randomly and replaced with sodium ions. The DMPG and DMPS systems contained ≈4200 and ≈4700 water molecules, respectively. The water layer corresponds to a hydration of ≈33 and ≈36 water molecules per lipid for the DMPG and DMPS bilayers, respectively.

For the simulations, the MD program NAMD [52] was used with the CHARMM27 all hydrogens parameter set and with the TIP3 water model [54]. The simulations were carried out in an *NPT* ensemble (i.e., constant number of atoms (*N*), temperature (*T*) and pressure (*P*)). The temperatures were 330 K (297 K) and 340 K (309 K) for DMPG and DMPS systems, respectively. The temperatures given in parentheses correspond to the gel–fluid phase transition temperatures of the different bilayer systems (LIPIDAT ID numbers: 3865 (DMPG), 2553 (DMPS); [55]). Generally, the finite size of a system and the order of phase transition may cause a broadening of the transition [56,57]. Kinnunen and co-workers [58] have recently suggested that the first-order gel–fluid phase transition of DPPC might additionally involve an intermediate phase that transforms into the liquid disordered phase as a second-order process. For second-order phase transition, the formation of co-operative, correlated motions with limited range broadens the main melting transition [59]. We have therefore chosen a temperature, which is relatively far away from the transition temperature to ensure that the bilayers are in the fluid-phase. A constant ambient pressure of 1 atm was imposed using the Langevin piston method [60] with a damping coefficient of 5 ps^{-1}, a piston period of 100 fs, and a decay of 50 fs. The Particle Mesh Ewald (PME) method was used for computation of the electrostatic forces [61,62]. The grid spacing applied was approximately 1.0 Å and a fourth order spline was used for the interpolation. The long range part of the electrostatic forces was evaluated every fourth femtosecond. Van der Waals interactions were cut off at 12 Å using a switching function starting at 10 Å. Periodic boundary conditions were imposed in all directions. Initially, the systems were energy minimised for 5000 steps, which was followed by 100 ps of heating of the systems to the desired temperature. A time step of 1 fs was used throughout all simulations. Simulations were performed for up to approximately 60 ns in an *NPT* ensemble. The analyses of the trajectory were performed using VMD [51].

Parameters for the PG and PS bilayers were taken from the CHARMM27 parameter set [63]. Missing parameters (bond-angles, dihedral angles, charges) for the PS head group were taken from the amino acid, serine. The charge distributions for the PG and PS head group regions were determined using an approach that was previously, successfully applied to a di-palmitoyl-phosphatidyl-choline bilayer and that was based on ab initio quantum mechanical calculations [64]. The charges were determined from ab initio calculations using the Restricted Hartree-Fock approximation with the 6–31+G* basis set followed by a Mulliken population analysis (charges are shown in Fig. 1). The calculations were performed within SPARTAN Version 1.0.2 (Wavefunction Inc., Irvine, California, USA).

2.2. Fluorescence measurements

1,2-dimyristoyl-*sn*-glycero-3-[phospho-rac-(1-glycerol)] (Sodium Salt) (DMPG) was purchased from Avanti Polar Lipids (Alabaster, AL) and was used without further purification. 6-dodecanoyl-2-dimethylaminonaphthalene (Laurdan) was purchased from Molecular Probes (Eugene, OR). All solvents were spectroscopy grade.

An appropriate amount of DMPG was dissolved in a 9:1 mixture of chloroform:methanol, and warmed above 35 °C for one min to ensure the solution was clear before adding the Laurdan. Laurdan was dissolved in a 1:1 mixture of chloroform:methanol and added to the DMPG solution to give a membrane concentration of the probe of 0.15 mol% (probe:phospholipid=1.5:1,000). The sample was then dried at 40 °C under a stream of nitrogen gas and placed under vacuum overnight to remove the residual solvent. The dry lipids were dispersed in either ultrapure water (18.2 Ω cm) (Millipore, Billerica, MA), a $CaCl_2$ solution (0.1 mM Ca^{2+}), or a NaCl solution (0.1 mM Na^+) to a final lipid concentration of 10 mM. It is important to note that the DMPG source contains one Na^+ counterion per lipid molecule, resulting in additional 10 mM Na^+ content in the 10 mM lipid stock solution. The samples were then warmed to 60 °C for a minimum of 1 h and vortexed multiple times until the solutions looked evenly dispersed. No variability in the results was observed between different preparations. For the fluorescence measurements 2.4 ml of a 1:50 dilution aliquot (final lipid concentration 0.2 mM) was added to a cuvette placed in a temperature-controlled holder regulated by an external water bath. The dilutions were carried out using the respective 0.1 mM $CaCl_2$ and 0.1 mM NaCl solutions. After this dilution step, the ionic concentrations are (a) 0.2 mM Na^+ for the control, (b) 0.1 mM Ca^{2+}+0.2 mM Cl^-+0.2 mM Na^+ for the "plus Ca^{2+}" sample, and (c) 0.3 mM Na^++0.1 mM Cl^- for the "plus Na^+" sample. The sample was continually stirred using a magnetic stir bar. No buffering agent was added to the solutions in order to avoid introducing additional factors that could affect the comparison with the simulation results. The pH was measured for the 0.2 mM DMPG aliquots to be 8.3 for pure water, 7.2 for the plus Ca^{2+} sample, and 6.8 for the plus Na^+ sample. Therefore change in pH could not account for the differences in lipid packing observed in the presence of Ca^{2+} since similar changes in pH were measured for the Na^+ sample, which showed no difference in lipid packing compared to the control sample.

To study the polarity of the lipid interfaces, we used Laurdan, which is an amphiphilic fluorescence probe used to study the dipolar relaxation processes [65]. Laurdan possesses a dipole moment due to the partial charge separation between 2-dimethylamino and the 6-carbonyl residues which further increases upon excitation [65,66]. Laurdan is virtually insoluble in water, thus the generalised polarisation (GP, see below) arises entirely from the probes located into the membrane [67]. In lipid membranes the fluorescent moiety of Laurdan resides at the level of the glycerol backbone [66]. In solvents of high polarity, Laurdan shows a considerable shift of its emission spectrum to longer wavelengths due to dipolar relaxation processes [68]. When the local environment of Laurdan is a phospholipid phase, the emission depends strongly on the packing of the lipid chains. At temperatures below the phase transition (gel state) the emission maximum is near 440 nm. At temperatures above the phase transition (liquid crystalline state) the emission maximum is red-shifted to ~490 nm [66,69]. In phospholipid membranes, the solvent dipolar relaxation process is independent of the type of polar headgroup and of pH within the range pH 4–10 [68,70]. GP quantitatively relates these spectral changes by taking into account the relative fluorescence intensities of the blue and red edge regions of the emission and excitation spectra, respectively [66,69]. The dipolar relaxation observed during membrane local bending fluctuations, membrane permeability, or phospholipid phase transition is due to the water molecules penetrating into the glycerol backbone level, and changing the dipolar relaxation of the Laurdan probe [66,68]. The higher the GP value, the lower the penetration [66,68,71,72]. Steady-state emission spectra were measured on a SLM DMX 8100 spectrofluorometer equipped with a Xenon-arc lamp (SLM-AMINCO, Urbana, IL) at 37 °C and 57 °C. The emission bandpass was set at 2 nm. The excitation wavelength was 340 nm. Generalised polarisation values were calculated from the emission spectra as follows [68]:

$$GP = \frac{I_B - I_R}{I_B + I_R}$$

where I_B and I_R is the emission intensity at 440 nm and 490 nm, respectively. Three to six samples were averaged for every data point. Samples were allowed to equilibrate for 15 min at the temperature of interest before collecting the spectra.

3. Results and discussion

Membranes are complex biological systems with many structural and dynamic properties that evolve at different time and length scales [73]. Therefore, simulations of these systems are a challenging task, which requires extensive computational calculations [23,24]; in particular when complexity is increased by for instance studying the properties of mix-bilayers, the interactions

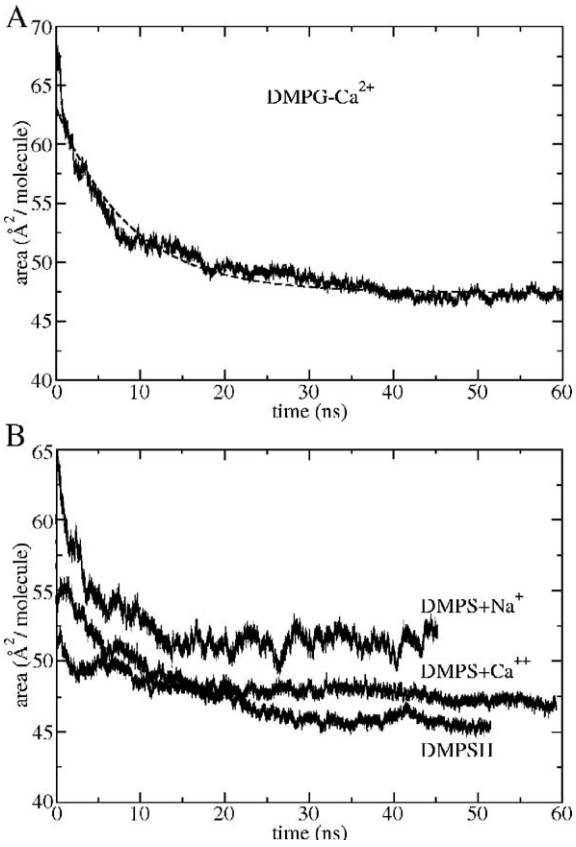

Fig. 2. Area per lipid molecule as a function of simulation time for bilayers of: Panel A) di-myristoyl-phosphatidyl-glycerol/calcium ions (DMPG–Ca^{2+}); Panel B) di-myristoyl-phosphatidyl-serine/calcium or sodium ions (DMPS–Ca^{2+} or DMPS–Na^{+}) and protonated di-myristoyl-phosphatidyl-serine, DMPSH. The functions were fitted with an exponential function (area=a_0+a_1 exp(−time/a_3)) to estimate the equilibrium area per molecule. The fitting function were: area(DMPG–Ca^{2+})=47.4+15.7exp(−time/8.5); area(DMPS–Ca^{2+})=47.3+3.1exp(−time/14.0); area(DMPS–Na^{+})=51.3+4.8*exp(−time/5.2); area(DMPSH)=45.3+10.0exp(−time/12.3).

of small molecules or proteins with membranes or the function of transmembrane proteins imbedded in a lipid bilayer. The complexity is even further increased when considering charged phospholipids, since positively charged counterions interact with the negatively charged lipids. Indeed, it has been experimentally observed that ions have an effect on the structural properties of bilayers and can induce phase transitions in bilayers [74,75]. Divalent cations play an important role in biological processes [76–80], and, when adsorbed onto a negatively charged membrane, significantly enhance the membrane stability by reducing the surface charge density and inducing a tighter packing of the phospholipids [81–83]. Hence, when studying complex systems such as the association of proteins or small molecules to charged membranes, the effect of counterions has to be taken into account, since the protein has to displace interfacially located ions before it can reach the membrane surface.

3.1. Lipid area

The time evolutions of the area per molecule for the different bilayers are shown in Fig. 2. In the presence of calcium ions, there is essentially no difference in the area per molecule between the different negatively charged bilayers. An increase in the area per molecule (≈4 $Å^2$) is observed for DMPS, when sodium ions are present. As we show below, this effect is due to a broader distribution of sodium ions at the membrane surface. The areas per molecule are 47.4±0.5 $Å^2$ (DMPG–Ca^{2+}), 47.3±0.5 $Å^2$ (DMPS–Ca^{2+}), 51.3±1.0 $Å^2$ (DMPS–Na^{+}) and 45.3±0.5 $Å^2$ (DMPSH).

3.2. Order parameter

The order of the acyl chains were deduced from the carbon–deuterium order parameter (S_{CD}) calculated using

$$S_{CD} = \langle 3/2(\cos^2\theta)-1/2\rangle, \quad (1)$$

where θ is the angle between the carbon–deuterium bond and the bilayer normal [84]. In the calculations, S_{CD} corresponds to the carbon–hydrogen bond. ⟨…⟩ implies an average over time and molecules. Fig. 3 shows the order parameters for DMPG, DMPS and DMPSH bilayers. The order parameters for the equilibrated negatively charged bilayers in the presence of Ca^{2+} are significantly higher than for zwitterionic PC-bilayers [28,85] suggesting that counterion-lipid molecule interactions increase the ordering in the anionic bilayers. Higher order was also observed in previous simulations of phosphatidyl-serine bilayers [27], where the reported order parameters were similar to our results. As shown in Fig. 3, in the presence of calcium ions, the order parameters for DMPS are similar to those for DMPG. Small differences are observed between carbon numbers 11–13, where the DMPS bilayer is slightly more ordered than the DMPG bilayer. As discussed below, in contrast to DMPG, DMPS has a carboxylate group that provides an additional interaction site for Ca^{2+}, and DMPS can also interact with the NH_3^+ group of neighbouring lipid molecules, thereby increasing molecular packing. In accordance with the area per molecule (Fig. 2), the ordering of DMPS is lower in the presence of sodium than of calcium counterions. However the

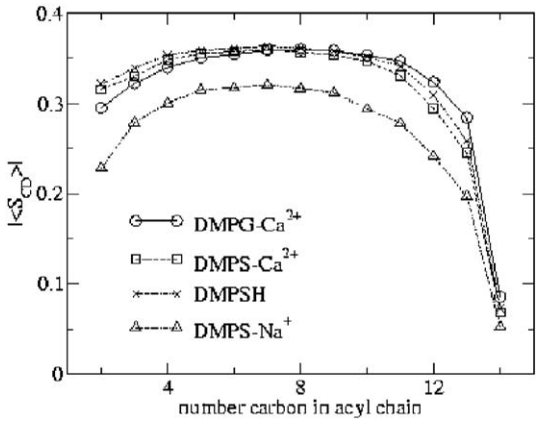

Fig. 3. Order parameter profiles for di-myristoyl-phosphatidyl-glycerol/calcium ions (DMPG–Ca^{2+}), di-myristoyl-phosphatidyl-serine/calcium or sodium ions (DMPS–Ca^{2+} or DMPS–Na^{+}) and protonated di-myristoyl-phosphatidyl-serine (DMPSH) bilayers. The order parameters were calculated applying Eq. (1). The first 25 ns of the trajectories were not used in these calculations.

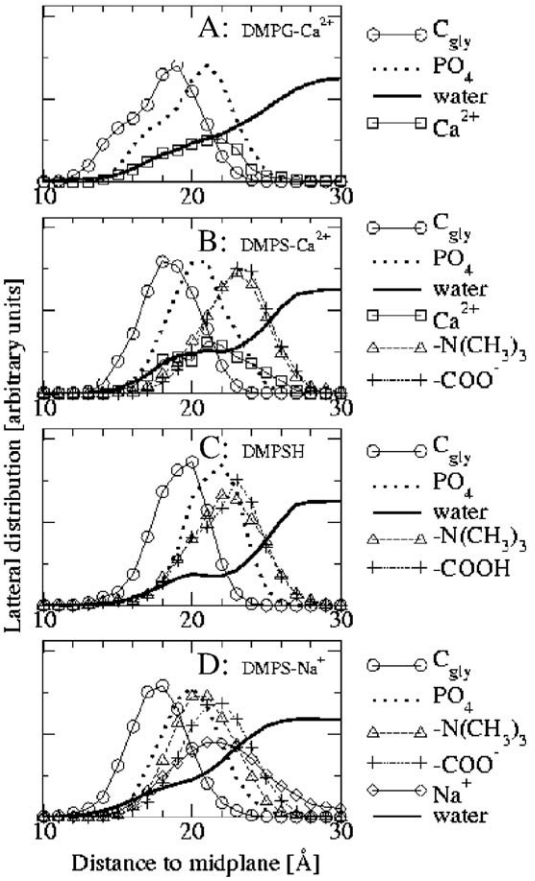

Fig. 4. Density distribution of selected atoms (indicated to the right) along the bilayer normal in DMPG–Ca^{2+} (A), DMPS–Ca^{2+} (B), DMPSH (C) and DMPS–Na^{+} (D). C_{gly} corresponds to the glycerol carbon connected to the head group, PO_4^- to the phosphatidyl group, Ca^{2+} refers to the calcium ion, $N(CH_3)^+$ refers to the choline group, COO^- refers to the carbon atom in the terminal carboxylate group in DMPS, and COOH refers to the protonated carboxylate group in DMPSH. Hydrophobic thicknesses specified by the transmembrane P–P distance are 41.3 Å, 42.0 Å, 43.6 Å and 40.6 Å respectively, for DMPG–Ca^{2+}, DMPS–Ca^{2+}, DMPSH and DMPS–Na^{+}.

order parameter observed are still higher than for PC bilayers in the fluid-phase [28,85].

3.3. Ion distribution

The electrostatic properties of the membrane interface are of paramount importance for a number of processes including neural transmission, membrane fusion, cell excitation and the adsorption of charged species to the membrane. These properties are strongly affected by charged lipids and counterions. Calcium is particularly interesting in this respect due to its divalent nature, and its important role in a large variety of signalling events. Ca^{2+} has been shown to be important in vivo for the processes listed above, and it has also been demonstrated to interact strongly with negatively charged model membranes [83,86–89]. The current results suggest that calcium ions move rapidly to the interface of both DMPG and DMPS bilayers. Thus, analysis of the time evolution of the coordination of Ca^{2+} (which are initially in the bulk phase of water) by respectively water and lipid (*c.f.* [90]) suggested steady state in the ion distribution was achieved in ~25 ns (data not shown). This information corroborates the relaxation time for the surface area derived from Fig. 2 and consequently we henceforth restrict our analysis to simulation times larger than 25 ns. This equilibration time is much faster than that observed for cations in zwitterionic bilayer systems. Boeckmann et al. reported that in zwitterionic bilayers with divalent salt the equilibration is between 100–200 ns [90]. In our simulations, calcium ions were found to be practically locked in the interfacial region subsequent to their adsorption. Thus, no calcium was found in the aqueous bulk

Table 1
Frequency distribution (in %) of charge–charge interactions in DMPG, DMPS and DMPSH

	0	1	2						
A									
Phosphatidyl	16	62	23						
Hydroxyl	77	16	7						
Ester carboxyl	99	1							
B									
Phosphatidyl	28	52	20						
Carboxylate	40	48	12						
Ester carboxyl	91	9							
C									
Phosphatidyl	56	38	6						
Carboxyl acid	95	5							
Ester carboxyl	87	13							
	0	1	2	3	4	5	6	7	8
D									
Lipid		5	30	53	11	2			
Total							78	20	2
E									
Lipid		2	9	44	33	13			
Total					3	8	69	20	
	0	1	2	3	4				
F									
DMPS	37	32	21	8	2				
DMPSH	17	30	34	16	3				

The data are given in percent and the cut-off length is set to 3 Å. (A) shows data for the Ca^{2+}–DMPG system. Three different moieties of the lipid (phosphatidyl, hydroxyl and ester oxygen) are considered. The first row, for example, shows that 16% of the phosphate ions are not within 3 Å of a calcium ion, while 62% and 23% of the phosphate coordinate 1 and 2 calcium ions, respectively. (B) illustrates analogous data for the DMPS–Ca^{2+} system. In this case, the moieties of the lipid considered are the two anions (phosphatidyl and carboxylate) and the ester oxygen. (C) lists the frequency of contacts of the proton on the carboxyl acid and selected groups. It appears that the proton is much less coordinating than the calcium ion.
(D) and (E) provide an overview of calcium ion coordination at the interface of DMPG and DMPS membranes, respectively. The tables list the number of lipids coordinating Ca^{2+} and the total coordination number (lipid+water). Inspection of the total coordination reveals that the majority of the ions are hexa-coordinated for both membranes. A coordination number of seven occurs at a frequency of 20% for both types of membranes, while other coordination numbers are negligible. The majority of calcium ions bind to 2–4 (moieties of) lipid molecules, and it follows that the hydration of bound calcium typically involves 2–4 water molecules.
Finally, (F) lists the frequency of choline groups that are directly bound to a phosphatidyl group in respectively DMPS and DMPSH membranes. It appears that 34 % of the phosphatidyl groups in DMPSH are directly bound to two choline groups while it is only 21 % for DMPS.

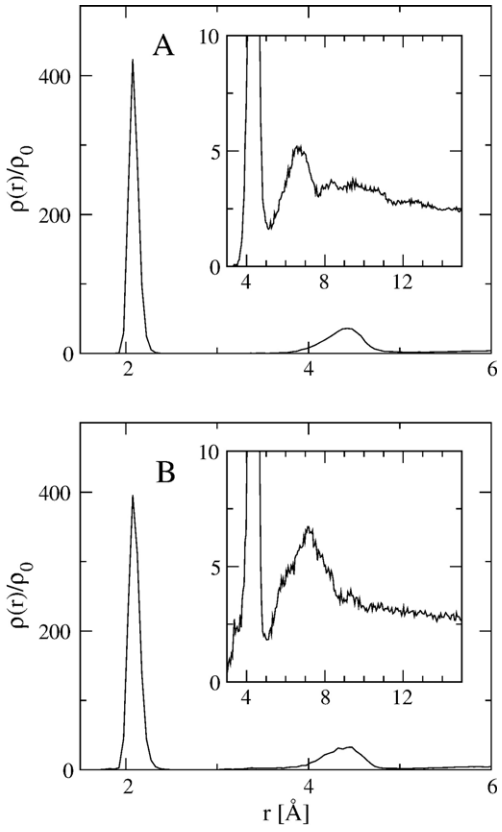

Fig. 5. Radial distribution function calculated between calcium ions and oxygen atoms in the phosphate group in DMPG–Ca^{2+} bilayer (A) or oxygen in the phosphate group in DMPS–Ca^{2+} bilayer (B). The inset in each panel is an enlargement of the distribution function between 3 and 15 Å.

towards the end of the simulations, and the diffusion coefficient extracted from the long-time limit of the time evolution of the mean squared displacement was approximately 6×10^{-7} cm^2/s. This is two order of magnitude lower than for bulk water. Moreover, the displacement of Ca^{2+} is equivalent to the root mean squared displacement (rmsd) of the phosphate atom indicating that calcium ions constitute an integral part of the membrane interface (on a ns time scale). Sodium ions are also observed in the interfacial regions of the DMPS–Na^+ system, but as discussed below show a broader distribution than calcium ions. This observation is in accord with two related simulation studies, which concluded that sodium ions intercalated into the interfacial region of phosphatidyl-serine membranes [19,27]. Comparison of these results points to some interesting differences between the two counterions. Primarily that calcium ions appear to be more strongly bound to the interfacial region than sodium ions. A stronger coordination of Ca^{2+} is also in accord with the observation that the ion populates a rather narrow (~10 Å) lateral plane at the membrane interface of PS membranes (Fig. 4), while the distribution of Na^+ at the interface is broader. Similarly, for palmitoyl-oleoyl phosphatidyl-serine bilayer [27], the distribution of sodium ions is about twice as broad as the distribution of calcium ions reported here. The broader distribution may be also explained by the conspicuous ability of the ester carbonyl groups to coordinate Na^+ [19,27], which allow a rather deep penetration of this counterion. In the case of calcium ions, contacts with the ester groups of DMPS are very rare (Table 1), and the interactions with phosphate and (to a lesser extent) carboxylate group in the head group region are predominant.

Calcium ions play an important role as a second messengers during signal transduction events. We therefore focussed in our further analysis on the structural properties of the phospholipid–Ca^{2+} complex. Structural information can be deduced from radial distribution functions shown in Fig. 5. The peak at 2.2 Å corresponds to the direct contact of counterions and the oxygen atom of phosphate- or (for PS) the carboxylate group. The peak around 4.5 Å corresponds to the anionic group of a neighbouring lipid molecule or (for PS) the second negative charge of the same lipid head group. Typical examples of these interactions are illustrated in Fig. 6 for DMPG–Ca^{2+} and DMPS–Ca^{2+}. An overview of the Ca^{2+} coordination by lipid and/or water molecules is provided in Table 1. It appears that the coordination of Ca^{2+} by lipids is almost entirely due to interactions with the anionic groups, while interactions with the oxygen atoms of the ester groups are negligible. This observation is in accord with solvent relaxation measurement [91] as well as atomic absorption and FT-IR spectroscopy measurements [92]. These studies indicated that divalent ions strongly interacted with the phosphate group in phosphatidyl-glycerol membranes [91,92]. Hydration of bound Ca^{2+} ions is significant and typically involves 3–4 water molecules (Table 1). The degree of hydration of membrane bound Ca^{2+} counterions is larger than found for sodium ions, which coordinated 2–3 water molecules when they intercalated into the region around the ester group of a phosphatidyl-serine membrane [27].

3.4. Fluorescence measurements

We have used the fluorescence probe, Laurdan, to assess the effect of Ca^{2+} or Na^+ on the properties of DMPG membranes. The fluorescence probe changes its dipolar relaxation properties as water molecules penetrate the interfacial region of the bilayer

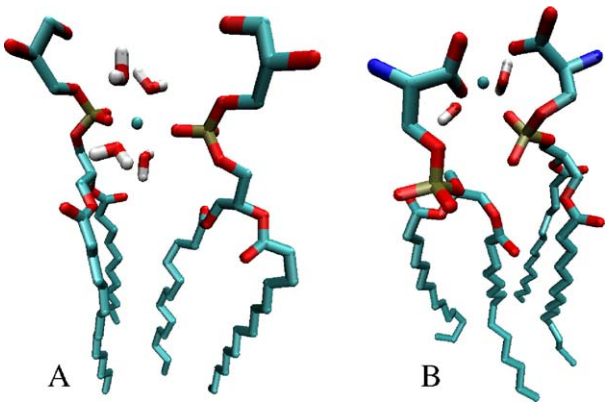

Fig. 6. Representative snapshots of Ca^{2+} ion coordination in DMPG bilayer (A) and DMPS bilayer (B). Coordination corresponds to a direct binding of Ca^{2+} to a lipid head group oxygen or water. In these examples, the Ca^{2+} ions bridge two lipid molecules. Statistical analysis (Table 1) showed that calcium most often coordinates three lipid moieties (Table 1D and E), emphasizing that bridging of two or more lipids is indeed prevalent.

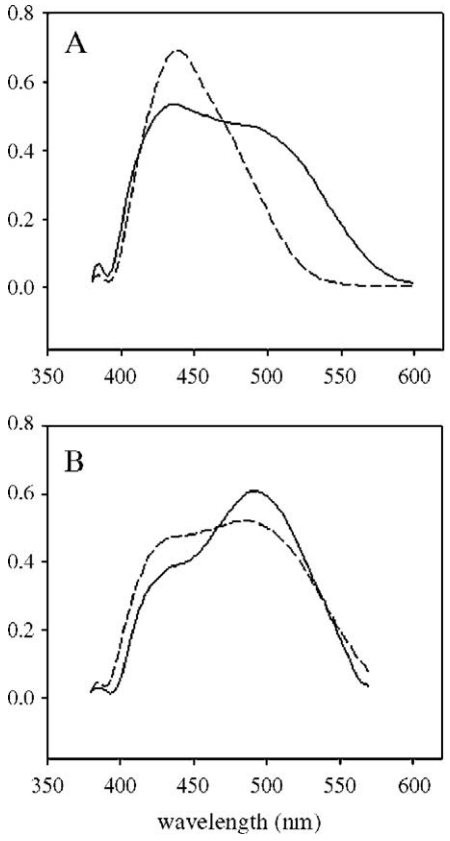

Fig. 7. Normalised emission spectra of Laurdan in DMPG multilamellar vesicles in the absence (solid line) and presence of 0.1 mM Ca^{2+} (dashed line) measured at (A) 37 °C and (B) 57 °C. The excitation wavelength was 340 nm.

[66,68]. Water intercalation depends on the state of the membrane, and hence the probe indirectly responses to, e.g., the packing of the membrane. The higher the GP value, the lower the penetration [66,68,71,72]. Fig. 7 shows the normalised emission spectra of Laurdan obtained for vesicles in no Ca^{2+} solution (solid line) and in 0.1 mM Ca^{2+} solution (dashed line) measured at two temperatures above the phase transition temperature. It should be noted that both samples contained 0.2 mM Na^+, which arises from Na^+ present in the DMPG stock (see Materials and methods). The increase in the emission maximum at approximately 440 nm due to the addition of Ca^{2+} is an indication that the polarity of the environment surrounding the probe has changed; i.e., the number and motional freedom of water molecules around the fluorescent group is reduced corresponding to an increase in lipid packing. In Fig. 8, the generalised emission polarisation (GP) values for Laurdan in DMPG vesicles at temperatures below (15 °C) and above (37 °C and 57 °C) the gel/liquid–crystalline phase transition are presented. At both temperatures corresponding to the fluid phase regime the presence of 0.1 mM Ca^{2+} (black) induces an increase in the GP value compared to no Ca^{2+} (white). The presence of an equivalent amount of Na^+ (grey) in addition to the 0.2 mM Na^+ content present in the control sample has no significant effect on the GP value. In accordance with the conclusions from our simulations, the fluorescence measurements clearly indicate that the effect of calcium on PG membrane systems is more pronounced than that of sodium.

3.5. Protonated DMPS bilayer

The lateral area per molecule of the simulated DMPG and DMPS membranes is significantly lower than the area per molecule of analogous zwitterionic membranes [28,85]. Since simple arguments based on charge repulsion among the lipid molecules might predict the opposite effect, the reduction in area again stresses the importance of lipid–counterion interactions. It suggests that the counterion–lipid complex is laterally more tightly packed than the zwitterionic lipids. This conclusion is further supported by the observation that both the acyl chain order parameter (Fig. 3) and the hydrophobic thickness (Fig. 4) are higher for the anionic lipids than for zwitterionic lipids [28]. An analogous "condensing" effect of counterions has previously been discussed for POPS–Na^+ and DPPS–Na^+ systems [19,27]. The area per molecule for DMPS–Ca^{2+} is about 4 $Å^2$ smaller than for DMPS–Na^+. This indicates that PS–Ca^{2+} (as well as PG–Ca^{2+}) interactions are characterised by a more significant increase in lateral packing of the respective lipid molecules in comparison to PG–Na^+ (see Fig. 8) or PS–Na^+ [19,27]. To investigate the significance of the negatively charged carboxylate group in PS on the binding of counterions, we performed a simulation where the carboxylate group was protonated. This bilayer (DMPSH) is zwitterionic in nature with a negatively charged phosphate group and a positive ammonium ion. Surprisingly, the area per molecule (Fig. 2B) and order parameter (Fig. 3) for DMPSH are, within the statistical error, the same as for the negatively charged PS bilayer with Ca^{2+} counterions. As indicated in Table 1, Ca^{2+}–PO_4^- / Ca^{2+}–COO^- electrostatic interactions (in PS systems) can be replaced by NH_3^+–PO_4^- interactions (present in DMPSH). The carboxylate groups in DMPSH are well exposed to the water phase and do not participate in lipid–lipid interactions (Table 1C). In DMPSH, interactions between the ammonium and phosphate moieties result in a network of strongly interacting lipid

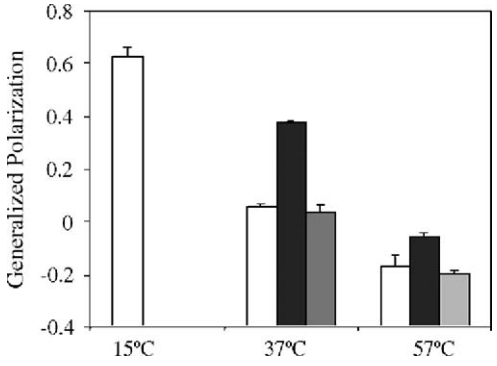

Fig. 8. Generalised polarisation (GP) values for Laurdan in DMPG multilamellar vesicles at temperatures below (15 °C) and above (37 °C and 57 °C) the gel/liquid–crystalline phase transition of DMPG. The GP values for a 0.2 mM Na^+ solution (white bar), a 0.1 mM Ca^{2+} + 0.2 mM Na^+ solution (black bar), and a 0.3 mM Na^+ solution (grey bar) are compared for the two temperature points above the phase transition temperature. The results show that the addition of Ca^{2+} increases the GP value of DMPG. An equivalent addition of Na^+ has no significant effect on the GP. The 0.2 mM Na^+ in the control arises from the stock lipid solution (see Materials and methods). The excitation wavelength was set at 340 nm, while the emission wavelengths were 440 nm and 490 nm.

molecules (Table 1). These interactions provide similar steric packing properties that lead to a comparable area per molecule. These different modes of interactions in respectively DMPSH and PS–Ca^{2+} hamper a direct discussion of Ca^{2+} effects based on comparisons of these two systems.

4. Conclusion

We have used molecular dynamics simulations to study the structure and dynamics of anionic bilayers, as well as to elucidate the effect of Ca^{2+} ions on the bilayer properties. The anionic bilayers consist of respectively di-myristoyl-phosphatidyl-glycerol (DMPG) and di-myristoyl-phosphatidyl-serine (DMPS). For comparison, we also included a di-myristoyl-phosphatidyl-serine bilayer, where the lipid molecules were protonated on the carboxylate group (DMPSH). For the negatively charged lipids, the areas per molecule are significantly lower than for analogous PC bilayers. The average areas were found to be 47.4±0.5 $Å^2$/molecule (DMPG with calcium), 47.3±0.5 $Å^2$/molecule (DMPS with calcium), 51.3±1.0 $Å^2$/molecule (DMPS with sodium) and 45.3±0.5 $Å^2$/molecule (DMPSH). The reduction in the areas is caused by the presence of counterions. Our results indicate that calcium ions are more strongly bound to the interfacial region than sodium ions and thereby inducing a "condensing effect" on the bilayer which is reflected in an increase in the acyl chain order parameter and hydrophobic thickness. This is in accordance with our fluorescence measurements which show that Ca^{2+} has a strong effect on PG membrane systems and that this effect is more pronounced for Ca^{2+} than for Na^+. Interestingly, our simulations show that the zwitterionic DMPSH bilayer is approximately as tightly packed as the negatively charged lipids with calcium as a counter ion. This is caused by strong interactions between the ammonium-phosphate moieties in DMPSH. The diffusion coefficient for Ca^{2+} is of the same order as for the phospholipids indicating that the calcium ions constitute an integral part of the membrane interface in the time window of our simulations. The pronounced effect of lipid–cation interactions found by this computational approach suggests that experimental studies of similar systems is of interest. Although precipitation of lipid–metal ion complexes may hamper such investigations [83], order parameters measured by NMR, area and thickness information measured by X-ray and neutron scatting techniques and packing properties derived from densitometry appear to be promising avenues towards an understanding of cation effects on charged membranes.

Acknowledgements

The authors acknowledge financial support from the Danish National Research Foundation via a grant to the MEMPHYS-Center for Biomembrane Physics. Additionally, GHP acknowledges financial support from the Danish Natural Science Research Council (project no.: 21-02-0488) and from the European's Sixth Framework program for Specific Targeted Research or Innovation Projects (BIOSCOPE, project no.: 505211-1). Simulations discussed here were performed at the Danish Center for Scientific Computing at the University of Southern Denmark.

References

[1] M. Edidin, Lipids on the frontier: a century of cell–membrane bilayers, Nat. Rev. Mol. Cell Biol. 4 (2003) 414–418.
[2] S.J. Singer, G.L. Nicolson, The fluid mosaic model of the structure of cell membranes, Science 175 (1972) 720–731.
[3] O.G. Mouritsen, Theoretical models of phospholipid phase transition, Chem. Phys. Lipids 57 (1991) 179–194.
[4] M. Edidin, Lipid microdomains in cell surface membranes, Curr. Opin. Struct. Biol. 7 (1997) 528–532.
[5] A. Kusumi, Y. Sako, Cell surface organization by the membrane skeleton, Curr. Opin. Cell Biol. 8 (1996) 566–574.
[6] A. Wisniewska, J. Draus, W.K. Subczynski, Is a fluid-mosaic model of biological membranes fully relevant? Studies on lipid organization in model and biological membranes, Cell. Mol. Biol. Lett. 8 (2003) 147–159.
[7] D. Rieman, G.H. Hansen, L.-L. Niels-Christiansen, E. Thorsen, L. Immerdahl, A.N. Santos, A. Kehlen, J. Langner, E.M. Danielsen, Caveolae/lipid rafts in fibroblast-like synoviocytes: ectopeptidase-rich membrane microdomains, Biochem. J. 354 (2001) 47–55.
[8] A. Caselli, B. Mazzinghi, G. Camici, G. Manao, G. Ramponi, Some protein tyrosine phosphatases target in part to lipid rafts and interact with caveolin-1, Biochem. Biophys. Res. Commun. 296 (2002) 692–697.
[9] L. Zhuang, J. Lin, M.L. Lu, K.R. Solomon, M.R. Freeman, Cholesterol-rich lipid rafts mediate Akt-regulated survival in prostate cancer cells, Cancer Res. 62 (2002) 2227–2231.
[10] G.S. Baron, Conversion of raft associated prion protein to the protease-resistant state requires insertion of PrP-res (PrP(Sc)) into continguous membranes, EMBO J. 21 (2002) 1031–1040.
[11] A. Kakio, S.-I. Nishimoto, K. Yanagisawa, Y. Kozutsumi, K. Matsuzaki, Interactions of amyloid beta-protein with various gangliosides in raft-like membranes: importance of GM1 ganglioside-bound form as an endogenous seed for Alzheimer amyloid, Biochemistry 41 (2002) 7385–7390.
[12] D. Duque, X.-J. Li, K. Katsov, M. Schick, Molecular theory of hydrophobic mismatch between lipids and peptides, J. Chem. Phys. 116 (2004) 10478–10484.
[13] F. Dumas, M.C. Lebrun, J.-F. Tocanne, Is the protein/lipid hydrophobic matching principle relevant to membrane organization and fluctuations? FEBS Lett. 458 (1999) 271–277.
[14] J.Y.A. Lehtonen, P.K.J. Kinnunen, Evidence for phospholipid microdomain formation in liquid crystalline liposomes reconstituted with *Escherichia coli* lactose permease, Biophys. J. 72 (2004) 1247–1257.
[15] S. Morein, R.E. Koeppe II, G. Lindblom, B. De Kruijff, J.A. Killian, The effect of peptide/lipid hydrophobic mismatch on the phase behavior of model membranes mimicking the lipid composition in *Escherichia coli* membranes, Biophys. J. 78 (2000) 2475–2485.
[16] G. Tans, J. Rosing, Snake venom activators of factor x: an overview, Haemostasis 31 (2001) 225–233.
[17] D. Marsh, L.I. Horvath, M.J. Swamy, S. Mantripragada, J.H. Kleinschmidt, Interaction of membrane-spanning proteins with peripheral and lipid-anchored membrane proteins: perspectives from protein–lipid interactions, Mol. Membr. Biol. 19 (2002) 247–255.
[18] J.-F. Tocanne, L. Cezanne, A. Lopez, B. Piknova, V. Schram, J.-F. Tournier, M. Welby, Lipid domains and lipid/protein interactions in biological membranes, Chem. Phys. Lipids 73 (1994) 139–158.
[19] S.A. Pandit, M.L. Berkowitz, Molecular dynamics simulation of dipalmitoylphosphatidylserine bilayer with Na^+ counterions, Biophys. J. 82 (2002) 1818–1827.
[20] M.I. Wallace, J.E. Molly, D.R. Trentham, Combined single-molecule force and fluorescence measurements for biology, J. Biol. 2 (2003) 1–5.
[21] M. Rief, H. Grubmüller, Force spectroscopy of single molecules, Chem. Phys. Chem. 3 (2002) 255–261.
[22] D.P. Tieleman, S.J. Marrink, H.J.C. Berendsen, A computer perspective of membranes: molecular dynamics studies of lipid bilayer systems, Biochim. Biophys. Acta 1331 (1997) 235–270.
[23] G.H. Peters, Computer simulations: a tool for investigating the function of complex biological macromolecules, in: A. Svendsen (Ed.), Enzyme Functionality: Design, Engineering, and Screening, Marcel Dekker, Inc., New York, 2004, pp. 97–147.

[24] T. Schlick, R.D. Skeel, A.T. Brunger, L.V. Kale, J.A. Board, J. Hermans, K. Schulten, Algorithmic challenges in computational molecular biophysics, J. Comput. Phys. 151 (1999) 9–48.
[25] M. Tarek, K. Tu, M.L. Klein, D.J. Tobias, Molecular dynamics simulations of supported phospholipid/alkanethiol bilayers on a gold(111) surface, Biophys. J. 77 (1999) 964–972.
[26] R.A. Böckmann, A. Hac, T. Heimburg, H. Grubmüller, Effect of sodium chloride on a lipid bilayer, Biophys. J. 85 (2003) 1647–1655.
[27] P. Mukhopadhyay, L. Monticelli, D.P. Tieleman, Molecular dynamics simulation of a palmitoyl-oleoyl phosphatidylserine bilayer with Na^+ counterions and NaCl, Biophys. J. 86 (2004) 1601–1609.
[28] M.Ø. Jensen, O.G. Mouritsen, G.H. Peters, Simulations of a membrane-anchored peptide: structure, dynamics, and influence on bilayer properties, Biophys. J. 86 (2004) 3556–3575.
[29] B.W. Lee, R. Faller, A.K. Sum, I. Vattulainen, M. Patra, M. Karttunen, Structural effects of small molecules on phospholipid bilayers investigated by molecular simulations, Fluid Phase Equilib. 225 (2004) 63–68.
[30] E. Falck, M. Patra, M. Karttunen, M. Hyvonen, I. Vattulainen, Membranes—lessons of sclicing membranes: interplay of packing, free area, and lateral diffusion in phospholipid/cholesterol bilayers, Biophys. J. 87 (2004) 1076–1091.
[31] C. Hofsass, E. Lindahl, O. Edholm, Molecular dynamics simulations of phospholipid bilayers with cholesterol, Biophys. J. 84 (2003) 2192–2206.
[32] S.A. Pandit, E. Jakobsson, H.L. Scott, Simulation of the early stages of nano-domain formation in mixed bilayers of sphingomylein, cholesterol, and dioleylphosphatidylcholine, Biophys. J. 87 (2004) 3312–3322.
[33] S.W. Chiu, E. Jakobsson, R.J. Mashl, H.L. Scott, Cholesterol-induced modifications in lipid bilayers: a simulation study, Biophys. J. 83 (2002) 1842–1853.
[34] A.M. Smondyrev, M.L. Berkowitz, Molecular dynamics simulation of the structure of dimyristoylphosphatidylcholine bilayers with cholesterol, ergosterol, and lanosterol, Biophys. J. 80 (2001) 1649–1658.
[35] K. Tu, M.L. Klein, D.J. Tobias, Constant-pressure molecular dynamics investigation of cholesterol effects in a dipalmitoylphosphatidylcholine bilayer, Biophys. J. 75 (1998) 2147–2156.
[36] C.S. Pereira, R.D. Lins, I. Chandrasekhar, L.C.G. Freitas, P.H. Hünenberger, Interaction of the disaccharide trehalose with phospholipid bilayer: a molecular dynamics study, Biophys. J. 86 (2004) 2273–2285.
[37] A. Grottesi, C. Domene, S. Haider, M.S.P. Sansom, Molecular dynamics simulation approaches to K channels: conformational flexibility and physiological function, IEEE Trans. Nanobiosci. 4 (2005) 112–120.
[38] W.L. Ash, M.R. Zlomislic, E.O. Oloo, D.P. Tieleman, Computer simulations of membrane proteins, Biochim. Biophys. Acta 1666 (2004) 158–189.
[39] M.Ø. Jensen, S. Park, E. Tajkhorshid, K. Schulten, Energetics of glycerol conduction through aquaglyceroporin GlpF, Proc. Natl. Acad. Sci. U. S. A. 99 (2002) 6731–6736.
[40] B.L. De Groot, H. Grubmüller, Water permeation through biological membranes: mechanism and dynamics of aquaporin-1 and GlpF, Science 294 (2001) 2353–2357.
[41] J. Gullingsrud, K. Schulten, Lipid bilayer pressure profiles and mechanosensitive channel gating, Biophys. J. 86 (2004) 3496–3509.
[42] S. Stoilova-McPhie, B.O. Villoutreix, K. Mertens, G. Kernball-Cook, A. Holzenburg, 3-Dimensional structure of membrane-bound coagulation factor VIII: modeling of the factor VIII heterodimer within a 3-dimensional density map derived by electron crystallography, Blood 99 (2002) 1215–1223.
[43] J.E. Cronan, Baterial membrane lipids: where do we stand? Annu. Rev. Microbiol. 57 (2003) 203–224.
[44] G. Devendra, R.G. Spragg, Lung surfactant in subacute pulmonary disease, Respir. Res. 3 (2002) 19–22.
[45] A.G. Buckland, D.C. Wilton, Anionic phospholipids, interfacial binding and the regulation of cell functions, Biochim. Biophys. Acta 1483 (2000) 199–216.
[46] M. Hallman, L. Gluck, Phosphatidylglycerol in lung surfactant. III: possible modifier of surfactant function, J. Lipid Res. 17 (1976) 257–262.
[47] F.C. Tsui, D.M. Ojcius, W.L. Hubbell, The intrinsic pKa values for phosphatidylserine and phosphatidylethanolamine in phosphatidylcholine host bilayers, Biophys. J. 49 (1986) 459–468.
[48] H. Hauser, G.G. Shipley, Comparative structural aspects of cation binding to phosphatidylserine bilayer, Biochim. Biophys. Acta 813 (1985) 343–346.
[49] H. Hauser, G. Shipley, Interactions of monovalent cations with phosphatidylserine bilayer membranes, Biochemistry 22 (1983) 2171–2178.
[50] G. Cevc, A. Watts, D. Marsh, Titration of the phase transition of phophatidylserine bilayer membranes. Effects of pH, surface electrostatics, ion binding, and head-group hydration, Biochemistry 20 (1981) 4955–4965.
[51] W. Humphrey, A. Dalke, K. Schulten, VMD—Visual molecular dynamics, J. Mol. Graph. 14 (1996) 33–38.
[52] L. Kale, R. Skeel, M. Bhandarkar, R. Brunner, A. Gursoy, N. Krawetz, J. Phillips, A. Shinozaki, K. Varadarajan, K. Schulten, NAMD2: greater scalability for parallel molecular dynamics, J. Comput. Phys. 151 (1999) 283–312.
[53] SOLVATE, (2005), http://www.mpibpc.gwdg.de/abteilungen/071/solvate/docu.html.
[54] W.L. Jorgensen, J. Chandrasekhar, J.D. Medura, R.W. Impey, M.L. Klein, Comparison of simple potential models for simulating liquid water, J. Chem. Phys. 79 (1983) 926–935.
[55] LIPIDAT, (2005), http://www.lipidat.chemistry.ohio-state.edu.
[56] T.L. Hill, Thermodynamics of small systems, J. Chem. Phys. 36 (1962) 3182–3197.
[57] T.L. Hill, R.V. Chamberlin, Extension of the thermodynamics of small systems to open metastable states: an example, Proc. Natl. Acad. Sci. U. S. A. 95 (1998) 12779–12782.
[58] A.J. Metso, A. Jutila, J.P. Mattila, J.M. Holopainen, P.K.J. Kinnunen, Nature of the main transition of dipalmitoylphosphocholine bilayers inferred from fluorescence spectroscopy, J. Phys. Chem. B 107 (2003) 1251–1257.
[59] T.M. Koyama, C.R. Stevens, E.J. Borda, K.J. Grobe, D.A. Clearly, Characterizing the gel to liquid crystal transition in lipid-bilayer model systems, Chem. Educ. 4 (1999) 12–15.
[60] S.E. Feller, Y. Zhang, R.W. Pastor, B.R. Brooks, Constant pressure molecular dynamics simulation—The Langevin piston method, J. Chem. Phys. 103 (1995) 4613–4621.
[61] U. Essmann, L. Perera, M.L. Berkowitz, T. Darden, H. Lee, L.G. Pedersen, A smooth particle mesh Ewald method, J. Chem. Phys. 103 (1995) 8577–8593.
[62] T. Darden, D. York, L. Pedersen, Particle mesh Ewald: an N log(N) method for Ewald sums, J. Chem. Phys. 98 (1993) 10089–10092.
[63] S.E. Feller, A. MacKerell, An improved empirical potential function for molecular simulations of phospholipids, J. Phys. Chem. B 104 (2000) 7510–7515.
[64] J. Sonne, F.Y. Hansen, G.H. Peters, Methodological problems in pressure profile calculations for lipid bilayers, J. Chem. Phys. 122 (2005) 1–9.
[65] G. Weber, F.J. Farris, Synthesis and spectral properties of a hydrophobic fluorescent probe: 6-propionyl-2-(dimethylamino)naphthalene, Biochemistry 18 (1979) 3075–3078.
[66] T. Parasassi, E.K. Krasnowska, L.A. Bagatolli, E. Gratton, Laurdan and Prodan as polarity-sensitive fluorescent membrane probes, J. Fluoresc. 8 (1998) 365–373.
[67] T. Parasassi, M. Loiero, M. Raimondi, G. Ravagnan, E. Gratton, Absence of lipid gel-phase domains in seven mammalian cell lines and in four primary cell types, Biochim. Biophys. Acta 1153 (1993) 143–154.
[68] T. Parasassi, G. De Stasio, G. Ravagnan, R.M. Rusch, E. Gratton, Quantitation of lipid phases in phospholipid vesicles by the generalized polarization of Laurdan fluorescence, Biophys. J. 60 (1991) 179–189.
[69] T. Parasassi, E. Gratton, Membrane lipid domains and dynamics as detected by Laurdan fluorescence, J. Fluoresc. 5 (1995) 59–69.
[70] T. Söderlund, J.-M.I. Alakoskela, A.L. Pakkanen, P.K.J. Kinnunen, Comparison of the effects of surface tension and osmotic pressure on the interfacial hydration of a fluid phospholipid bilayer, Biophys. J. 85 (2003) 2333–2341.
[71] T. Parasassi, M. Di Stefano, M. Loiero, G. Ravagnan, E. Gratton, Cholesterol modifies water concentration and dynamics in phospholipid bilayers: a fluorescence study using Laurdan probe, Biophys. J. 66 (1994) 763–768.
[72] J.C.M. Lee, R.J. Law, D.E. Discher, Bending contributions to hydration of phospholipid and block copolymer membranes: unifying correlations

between probe fluorescence and vesicle thermoelasticity, Langmuir 17 (2001) 3592–3597.
[73] O.G. Mouritsen, K. Jørgensen, Small-scale lipid–membrane structure: Simulation versus experiment, Curr. Opin. Struc. Biol. 7 (1997) 518–527.
[74] H. Hauser, G. Shipley, Interactions of divalent cations with phosphatidylserine bilayer membranes, Biochemistry 23 (1984) 34–41.
[75] A. Watts, K. Harlos, D. Marsh, Charge-induced tilt in ordered-phase phosphatidylglycerol bilayers. Evidence from X-ray diffraction, Biochim. Biophys. Acta 645 (1981) 91–96.
[76] R. Bertram, G.D. Smith, A. Sherman, Modelling study of the effects of overlapping Ca(2+) microdomains on neurotransmitter release, Biophys. J. 76 (1999) 735–750.
[77] B.J. Ravoo, W.D. Weringa, J.B.F.N. Engberts, Membrane fusion in vesicles of oligomerizable lipids, Biophys. J. 76 (1999) 374–386.
[78] D.P. Chen, Le Xu, A. Tripathy, G. Meissner, B. Eisenberg, Selectivity and permeation in calcium release channel of cardiac muscle: alkali metal ions, Biophys. J. 76 (1999) 1346–1366.
[79] P. Garidel, C. Johann, A. Blume, Thermodynamics of lipid organization and domain formation in phospholipid bilayers, J. Liposome Res. 10 (2000) 131–158.
[80] I. Ubarretxena-Belandia, R.C. Cox, R. Dijkman, M.R. Egmond, H.M. Verheij, N. Dekker, Half-of-the-sites reactivity of outer membrane phopholipase A against an active-site directed inhibitor, Eur. J. Biochem. 260 (1999) 794–800.
[81] Y.W. Kim, W. Sung, Effects of charge fluctuations on two-membrane instability and fusion, Phys. Rev. Lett. 91 (2003) 118101-1–118101-4.
[82] B.Y. Ha, Stabilization and destabilization of cell membranes by multivalent ions, Phys. Rev. E Stat. Phys. Plasmas Fluids Relat. Interdiscip. Topics 64 (2001) 051902-1–051902-5.
[83] P. Garidel, G. Förster, W. Richter, B.H. Kunst, G. Rapp, A. Blume, 1,2-Dimyristol-*sn*-glycero-3-phosphoglycerol (DMPG) divalent cation complexes: an X-ray scattering and freeze-fracture electron microscopy study, Phys. Chem. Chem. Phys. 2 (2000) 4537–4544.
[84] B.W. Koenig, H.H. Strey, K. Gawrisch, Membrane lateral compressibility determined by NMR and X-ray diffraction: Effect of acyl chain polyunsaturation, Biophys. J. 73 (1997) 1954–1966.
[85] J.F. Nagle, S. Tristram-Nagle, Structure of lipid bilayers, Biochim. Biophys. Acta 1469 (2000) 159–195.
[86] P. Garidel, A. Blume, Interaction of alkaline earth cations with the negatively charged phospholipid 1,2-dimyristoyl-*sn*-glycero-3-phosphoglycerol: a differential scanning and isothermal titration calorimetric study, Langmuir 15 (1999) 5526–5534.
[87] P. Garidel, A. Blume, W. Hübner, A Fourier transform infrared spectroscopic study of the interaction of alkaline earth cations with the negatively charged phospholipid 1,2-dimyristoyl-*sn*-glycero-3-phosphoglycerol, Biochim. Biophys. Acta 1466 (2000) 245–259.
[88] H. Binder, G. Köhler, K. Arnold, O. Zschörnig, pH and Ca2+ dependent interaction of Annexin V with phospholipid membranes: a combined study using fluorescence techniques, microelectrophoresis and infrared spectroscopy, Phys. Chem. Chem. Phys. 2 (2000) 4615–4623.
[89] J. Mattai, H. Hauser, R.A. Demel, G.G. Shipley, Interactions of metal ions with phosphatidylserine bilayer membranes: Effect of hydrocarbon chain unsaturation, Biochemistry 28 (1989) 2322–2330.
[90] R.A. Böckmann, H. Grubmüller, Multistep binding of divalent cations to phospholipid bilayers: A molecular dynamics study, Angew. Chem. Int. Ed. Engl. 43 (2004) 1021–1024.
[91] R. Hutterer, F.W. Schneider, W.Th. Hermens, R. Wagenvoord, M. Hof, Binding of prothrombin and its fragment 1 to phospholipid membranes studied by the solvent relaxation technique, Biochim. Biophys. Acta 1414 (1998) 155–164.
[92] M. Fragata, F. Bellemare, E.K. Nenonene, Mg(II) adsorption to a phosphatidylglycerol model membrane studied by atomic absorption and FT-IR spectroscopy, J. Phys. Chem. B 101 (1997) 1916–1921.